CrossMark

Moisture Absorption in Capillary Active Materials: Analytical Solution for a Multiple Step Diffusivity Function

Michele Bianchi Janetti[1] (ORCID)

Abstract

The absorption of moisture in a homogeneous, capillary active material obeys a diffusion law in which the driving potential is the volumetric water content, and the material behavior is characterized by the diffusivity function. In this study, an analytical solution for the one-dimensional case is proposed. The transient moisture profile is found by assuming the diffusivity as a multiple step function of the local water content and by solving the corresponding free boundary problem. Finally, a method for inverse determination of the diffusivity function is proposed. The case of a diffusivity function with three steps is investigated and discussed as an example.

Keywords Capillary active materials · Moisture absorption · Multiple step diffusivity · Free boundary problem

List of symbols

a_i; b_i	Functions Eqs. (21), (22) (m)
A	Absorbing surface (m^2)
$C_{i,1}$	Coefficients Eq. (16) ($\frac{\sqrt{s}}{m}$)
$C_{i,2}$	Coefficients Eq. (16) ($\frac{m^3}{m^3}$)
D	Diffusivity ($\frac{m^2}{s}$)
f	Function Eq. (29) (−)
g	Function Eq. (22) (−)
m	Mass (kg)
s	Integration variable ($\frac{m}{\sqrt{s}}$)
t	Time (s)
T	Absolute temperature (K)
u	Volumetric water content ($\frac{m^3}{m^3}$)
u_i^*	Limit water content ($\frac{m^3}{m^3}$)
x	Coordinate (m)

✉ Michele Bianchi Janetti
michele.janetti@uibk.ac.at

1   Unit for Energy Efficient Building, University of Innsbruck, Technikerstrasse 13, 6020 Innsbruck, Austria

x_i^* Free boundary position (m)
λ Boltzmann variable ($\frac{m}{\sqrt{s}}$)
λ_i^* Limit value of λ ($\frac{m}{\sqrt{s}}$)
ρ Density of water ($\frac{kg}{m^3}$)
Ψ Porosity ($-$)

Subscripts

$i = 1, \ldots, n$ Index
$k = 1, \ldots, n$ Index
0 Initial

1 Introduction

Isothermal absorption of moisture in unsaturated porous media is relevant in various fields of engineering as, e.g., building physics (Gummerson et al. 1980; Pel and Brocken 1996; Krus 1996; Roels et al. 2000; Carmeliet et al. 2004, 2007; Roels and Carmeliet 2006; Derluyn et al. 2013; Janetti and Wagner 2017) and earth sciences (Zimmerman and Bodvarsson 1989, 1991; Lockington 1993; Parlange et al. 1998). It has been shown that, under certain assumptions, the moisture transfer obeys a diffusion law in which the local moisture content is the driving potential, while the diffusivity is a function of the moisture content itself. This diffusion law is suitable to predict the transient moisture absorption in homogeneous, capillary active, construction materials and soils if gravity is negligible when compared to the capillary forces (Pel and Brocken 1996; Krus 1996; Carmeliet et al. 2004; Janetti and Wagner 2017).

While the above problem can easily be solved via numerical methods (Häupl et al. 1997; Künzel and Kiessl Oct 1996; Schijndel 2009; Janssen 2013), it may be a challenge to find a rigorous analytical solution since, as mentioned above, the diffusivity depends strongly on the moisture content. Various approximated solutions have been proposed mainly for applications in soil sciences by assuming simplified water content profiles depending on adjustable parameters (Zimmerman and Bodvarsson 1989, 1991; Parlange et al. 1998; Zhou 2014; Hristov 2016). The values of these parameters were then determined by requiring the assumed solution to satisfy an integral form of the equation which describes conservation of moisture.

Alternatively, an analytical solution can be found if the diffusivity is approximated by a step function of the water content. Solutions for a single step function are available in previous studies, as, e.g., Crank (1951, 1975) and Janetti and Wagner (2017). In Janetti and Wagner (2017), it is shown that this simplified model is adequate to reproduce the fundamental absorption behavior of certain building materials as, e.g., calcium silicate and ceramic brick, but it may be inaccurate in some other cases. In particular, the single step diffusivity may fail to represent accurately the water content profile near the absorbing face and in the nearly dry region. In this study, the solution proposed by Janetti and Wagner (2017) is extended to the case of a multiple step function which is able to approximate arbitrary curves and hence may be applied to a larger variety of real materials and absorption behaviors.

The solution proposed in the paper may be useful as a benchmark for numerical models, or for inverse determination of the diffusivity. Moreover, with respect to widespread numerical methods (e.g., finite element or finite difference methods), the proposed approach contains much less degrees of freedom since a few steps are in general sufficient to reproduce well the absorption behavior.

2 Description of the Method

We consider isothermal absorption in a material which can be assumed homogeneous at the macroscopic scale and where gravity is negligible when compared to the capillary forces. According to several authors (Gummerson et al. 1980; Pel and Brocken 1996 among others), the one-dimensional moisture transfer is described by the following diffusion equation, which is derived from the moisture balance on an infinitesimal element of volume:

$$\frac{\partial u}{\partial t} = \frac{\partial}{\partial x}\left(D(u)\frac{\partial u}{\partial x}\right) \tag{1}$$

Here u denotes the local volumetric water content (m^3/m^3) and $D(u)$ the diffusivity (m^2/s), while the initial and boundary conditions are given by the following equations:

$$u(0, x) = u_0 < 1 \tag{2}$$

$$u(t, 0) = 1 \tag{3}$$

$$\lim_{x \to \infty} u(t, x) = u_0 \tag{4}$$

To solve the problem given by Eqs. (1–4), the diffusivity $D(u)$, which characterizes the material behavior, has to be known. Experimental data (Pel and Brocken 1996; Carmeliet et al. 2004; Bianchi Janetti et al. 2016) show that this function presents generally a nearly exponential growth. In fact, approximated solutions for an exponential diffusivity curve have been already published in various studies (Zimmerman and Bodvarsson 1989, 1991; Parlange et al. 1998; Zhou 2014; Hristov 2016). In this paper, we shall follow a different approach by introducing a multiple step function defined as follows:

$$D(u) = \begin{cases} D_1 & : u < u_1^* \\ \vdots \\ D_i & : u_{i-1}^* < u < u_i^* \\ \vdots \\ D_n & : u_{n-1}^* < u \end{cases} \tag{5}$$

with the coefficients u_i^* denoting the water contents at which the diffusivity changes. This approach is profitable since it allows to describe arbitrary diffusivity functions. Even if $D_{i+1} > D_i$ holds in general, different configurations are possible, as explained later in the paper.

3 Analytical Solution

The analytical solution of the above problem for $n = 2$ has been presented by Crank (1951, 1975) and applied in Janetti and Wagner (2017) to reproduce the behavior of real building materials. In this paper, that solution is extended to the general case by dividing the domain into n regions in each of which the diffusivity may assume a different constant value as stated by Eq. (5). Accordingly, Eq. (1) can be rewritten as follows:

$$\frac{\partial u_i}{\partial t} = D_i \frac{\partial^2 u_i}{\partial x^2} \tag{6}$$

with $i = 1, \ldots, n$. The solution $u(t, x)$ of the original problem can hence be represented by n functions, valid in different regions delimited by the coefficients u_i^*:

$$u(t, x) = \begin{cases} u_1(t, x) & : u < u_1^* \\ \vdots \\ u_i(t, x) & : u_{i-1}^* < u < u_i^* \\ \vdots \\ u_n(t, x) & : u_{n-1}^* < u \end{cases} \tag{7}$$

The boundaries separating these regions evolve during time, and their positions are identified by $x_i^*(t)$, i.e.: $u(t, x_i^*(t)) = u_i^*$. Moreover, since the function $u(t, x)$ and the flux have to be continuous, the following conditions are satisfied:

$$u_i\left(t, x_i^*\right) = u_{i+1}\left(t, x_i^*\right) \tag{8}$$

$$D_i \frac{\partial u_i}{\partial x}\left(t, x_i^*\right) = D_{i+1} \frac{\partial u_{i+1}}{\partial x}\left(t, x_i^*\right) \tag{9}$$

To solve the above problem, the well-known Boltzmann transformation can be applied, as described, e.g., in Crank (1975). According to this approach, each solution of Eq. (6) is a function of a unique independent variable λ, defined as follows:

$$\lambda = \frac{x}{\sqrt{t}} \tag{10}$$

For simplicity and since no ambiguity is likely to occur, we use the same notation $u_i(\lambda)$ for the function $u_i(\lambda) = u_i(1, \lambda)$ of one variable. Thus, Eq. (6) can be reformulated as follows:

$$\frac{\lambda}{2} \frac{du_i(\lambda)}{d\lambda} + D_i \frac{d^2 u_i(\lambda)}{d\lambda^2} = 0 \tag{11}$$

with the boundary conditions:

$$\lim_{\lambda \to \infty} u_1(\lambda) = u_0 \tag{12}$$

$$u_n(0) = 1 \tag{13}$$

and continuity conditions:

$$u_i\left(\lambda_i^*\right) = u_{i+1}\left(\lambda_i^*\right) = u_i^* \tag{14}$$

$$D_i \frac{du_i}{d\lambda}\left(\lambda_i^*\right) = D_{i+1} \frac{du_{i+1}}{d\lambda}\left(\lambda_i^*\right) \tag{15}$$

where according to Eq. (10): $x_i^*(t) = \lambda_i^* \sqrt{t}$. The general solution of Eq. (11) is:

$$u_i(\lambda) = C_{i,1} \int_0^\lambda e^{-s^2/(4D_i)} ds + C_{i,2} \tag{16}$$

with

$$\int_0^\lambda e^{-s^2/(4D_i)} ds = \sqrt{D_i \pi} \, \text{erf}\left(\frac{\lambda}{\sqrt{4D_i}}\right) \tag{17}$$

Each solution $u_i(\lambda)$ holds in a different region $[\lambda_i^*, \lambda_{i-1}^*]$ with $\lambda_i^* < \lambda_{i-1}^*$, as shown in Fig. 1.
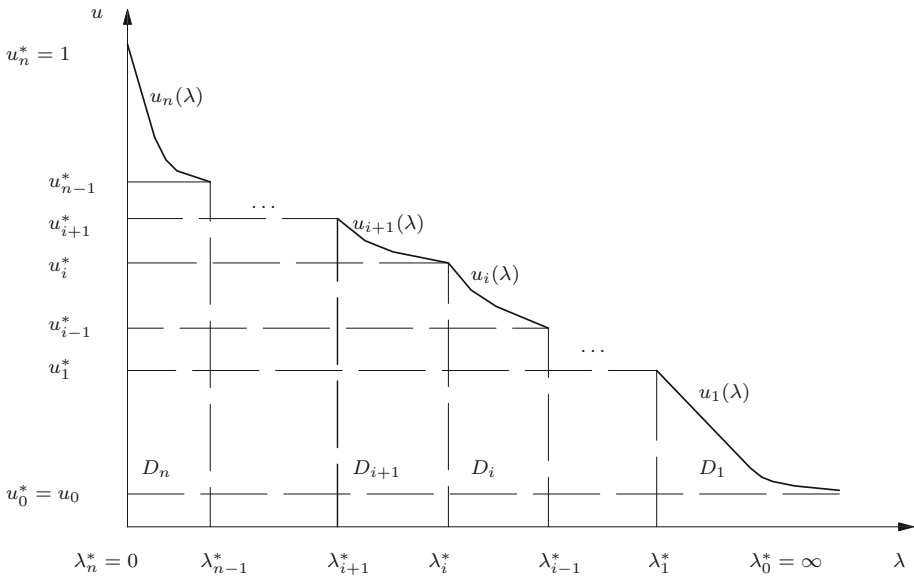
Fig. 1 Schematic representation of the curve $u(\lambda)$

The coefficients $C_{i,j}$ are determined by the boundary and continuity conditions as follows. From Eqs. (12–14) and (16), we obtain for $i = 1, \ldots, n$:

$$C_{i,1} = \frac{u_{i-1}^* - u_i^*}{\sqrt{D_i \pi} \left[\text{erf} \left(\frac{\lambda_{i-1}^*}{\sqrt{4D_i}} \right) - \text{erf} \left(\frac{\lambda_i^*}{\sqrt{4D_i}} \right) \right]} \tag{18}$$

$$C_{i,2} = u_{i-1}^* - C_{i,1} \sqrt{D_i \pi} \, \text{erf} \left(\frac{\lambda_{i-1}^*}{\sqrt{4D_i}} \right) \tag{19}$$

with $u_0^* = u_0$, $u_n^* = 1$, $\lambda_0^* = \infty$ and $\lambda_n^* = 0$. Considering Eq. (15) and the general solution expressed by Eq. (16), we can write $n - 1$ equations of the form:

$$D_i C_{i,1} e^{-\lambda_i^{*2}/(4D_i)} = D_{i+1} C_{i+1,1} e^{-\lambda_i^{*2}/(4D_{i+1})} \tag{20}$$

with $i = 1, \ldots, n - 1$. Note that for $n = 2$ one single equation remains, as considered in Janetti and Wagner (2017). By taking into account Eqs. (18–19), Eq. (20) can be rewritten as follows:

$$\underbrace{\frac{D_i \left(u_{i-1}^* - u_i^* \right) e^{-\lambda_i^{*2}/(4D_i)}}{\sqrt{D_i \pi} \left[\text{erf} \left(\frac{\lambda_{i-1}^*}{\sqrt{4D_i}} \right) - \text{erf} \left(\frac{\lambda_i^*}{\sqrt{4D_i}} \right) \right]}}_{a_i} = \underbrace{\frac{D_{i+1} \left(u_i^* - u_{i+1}^* \right) e^{-\lambda_i^{*2}/(4D_{i+1})}}{\sqrt{D_{i+1} \pi} \left[\text{erf} \left(\frac{\lambda_i^*}{\sqrt{4D_{i+1}}} \right) - \text{erf} \left(\frac{\lambda_{i+1}^*}{\sqrt{4D_{i+1}}} \right) \right]}}_{b_i} \tag{21}$$

To simplify the notation, the left- and right-hand sides of the equations above are denoted as a_i and b_i, respectively. In order to find the $n - 1$ coefficients λ_i^* which satisfy system (21), it is suitable to define the following function g:

$$g(\lambda_1, \ldots, \lambda_i, \ldots, \lambda_{n-1}) = \sum_{i=1}^{n-1} |a_i(\lambda_{i-1}, \lambda_i) - b_i(\lambda_i, \lambda_{i+1})|. \tag{22}$$

It is worth to note that the problem described by Eqs. (1–5) has one unique bounded solution $u(t, x) < 1$, as stated, e.g., in Barták et al. (1991), page 185. For this reason, we expect the function g to have one single root, which coincides with its minimum value, i.e., exists one unique lambda-set which satisfies the equation $g(\lambda_1, \ldots, \lambda_i, \ldots, \lambda_{n-1}) = 0$. Indeed, this root defines unequivocally the solution $u(t, x)$.

The coefficients λ_i^* can thus be determined by searching for the minimum of the function g. To this aim, a multidimensional optimization method, such as a direct search method (Lagarias et al. 1998; McKinnon 1998; Torczon 1997) or a Quasi-Newton method (Bonnans et al. 2006), can be used. Once the λ_i^* are known, the coefficients $C_{i,j}$ appearing in Eq. (16) are calculated through Eqs. (18–19).

In the following section, more details on the proposed method are given by considering a practical example.

4 Example for $n = 3$

In this section, the case of a diffusivity function having three steps ($n = 3$) is solved as an example. The solution $u(\lambda)$ is obtained as follows:

$$u(\lambda) = \begin{cases} u_1(\lambda) = C_{1,1}\sqrt{D_1\pi} \ \text{erf}\left(\dfrac{\lambda}{\sqrt{4D_1}}\right) + C_{1,2} \ : \lambda > \lambda_1^* \\[3mm] u_2(\lambda) = C_{2,1}\sqrt{D_2\pi} \ \text{erf}\left(\dfrac{\lambda}{\sqrt{4D_2}}\right) + C_{2,2} \ : \lambda_1^* > \lambda > \lambda_2^* \\[3mm] u_3(\lambda) = C_{3,1}\sqrt{D_3\pi} \ \text{erf}\left(\dfrac{\lambda}{\sqrt{4D_3}}\right) + C_{3,2} \ : \lambda_2^* > \lambda \end{cases} \qquad (23)$$

Here the coefficients $C_{i,j}$ are expressed by Eqs. (18–19), while λ_1^* and λ_2^* are determined by finding the minimum of the function, $g(\lambda_1, \lambda_2)$ expressed by Eq. (22) for $n = 3$. Despite its apparent simplicity, this model is able to reproduce a large variety of empirically observed absorption behaviors, as illustrated by the three representative cases discussed below.

The first case we consider regards a diffusivity function which steeply increases with the water content, as shown in Fig. 2a. As already noted above, this curve may well approximate the fundamental behavior of capillary active materials. The resulting moisture profiles are reported in Fig. 2b for three different initial values of the water content. Note that, according to Eq. (23), the function $u_1(\lambda)$ applies in the region of low water content (III), the function $u_2(\lambda)$ in the middle water content region (II) and the function $u_3(\lambda)$ in the region of high water content (I).

The second example taken into account refers to a diffusivity function which decreases when the water content approaches its maximum value, as shown in Fig. 3. This behavior was empirically observed in Carmeliet et al. (2004); Roels and Carmeliet (2006) and can be explained by considering that, in the nearly saturated region (I), the water transfer occurs mainly due to diffusion of entrapped air through the unsaturated material. This process is significantly slower than the capillary suction determining moisture transfer in the middle region (II), and hence results in a lower diffusivity in region I. It is worth to note, however, that the validity of Eq. (1) near to saturation is questionable. Carmeliet et al. (2004) observed that a purely diffusive approach may be inadequate in the nearly saturated region, since there a one-to-one relation between moisture potential (i.e., capillary pressure) and water content is not verified. Nevertheless, the diffusion equation seems to reproduce well the experimental data, as shown in Fig. 4. In this plot, the water content profiles deriving from different diffusivity
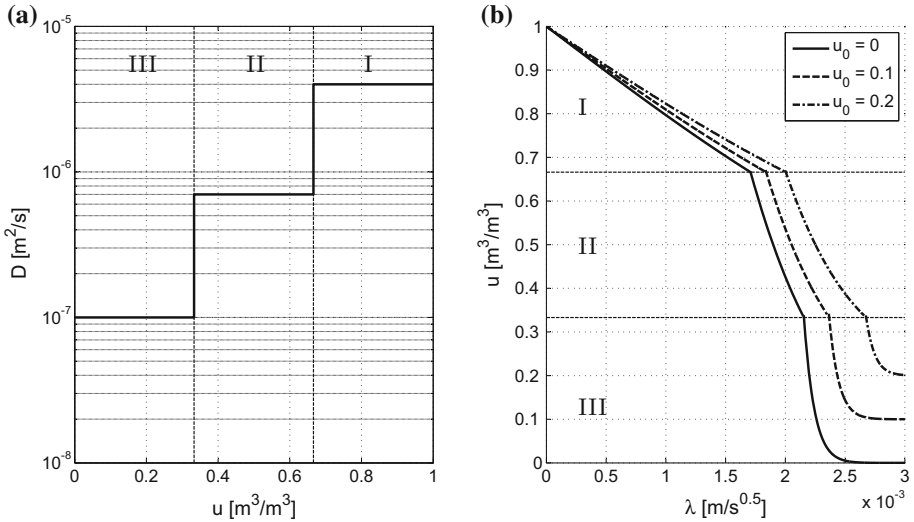
Fig. 2 **a** Increasing diffusivity function $D(u)$; **b** resulting water content profiles for three different initial values of the volumetric moisture content u_0
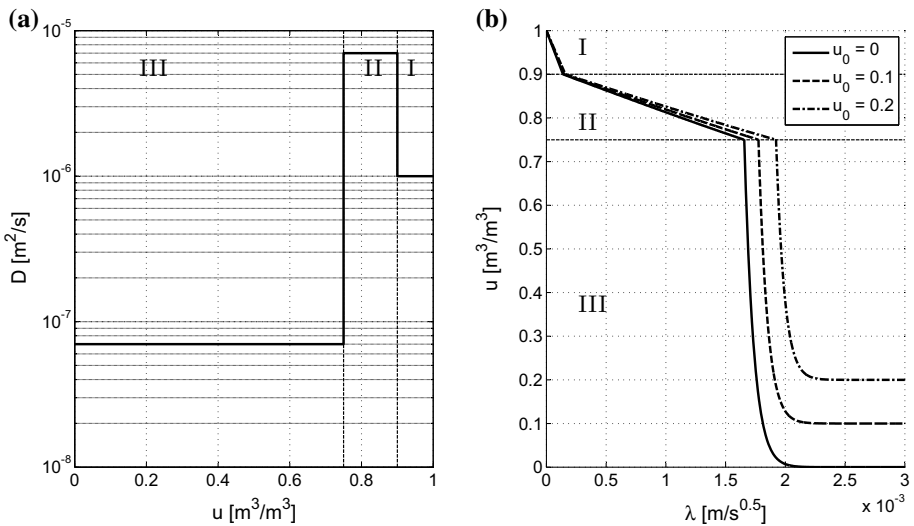

Fig. 3 **a** Diffusivity function $D(u)$ having a maximum in the middle region II; **b** resulting water content profiles for three different initial values of the volumetric moisture content u_0

functions are compared. In particular, two different multiple step functions ($n = 3$; $n = 6$) and a quasi-exponential curve are considered. The water content profile related to the quasi-exponential diffusivity has been obtained by numerical simulation.

In the last case investigated, which is reported in Fig. 5, the diffusivity is higher in the nearly dry region (III) than in the middle region (II). This effect can be explained by considering that, at low water content, vapor diffusion becomes decisive, leading to an increase in the total moisture transfer.
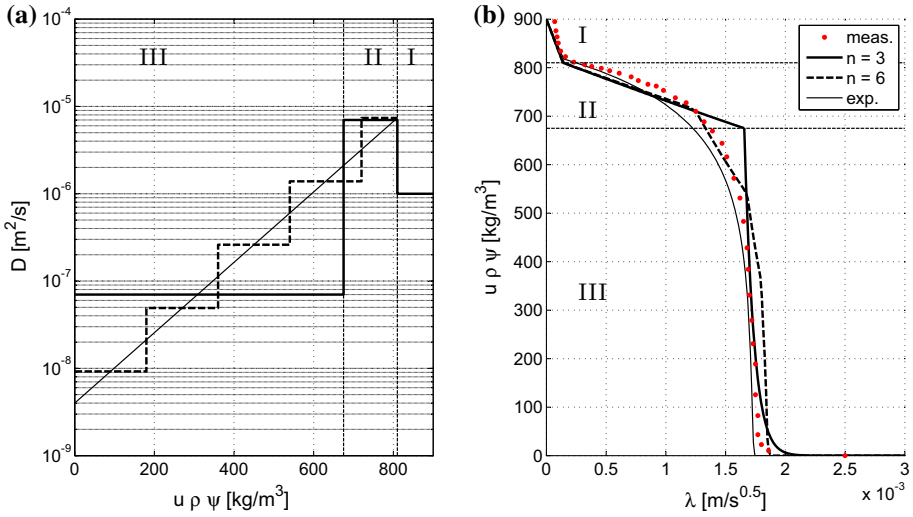
Fig. 4 a Diffusivity $D(u)$ approximated by different multiple step functions ($n = 3$ and $n = 6$) and by a quasi-exponential curve. The three curves are superimposed in region I; **b** resulting water content profiles and measured data by Carmeliet et al. (2004) [material: calcium silicate; $\rho \Psi = 900$ (kg/m^3)]
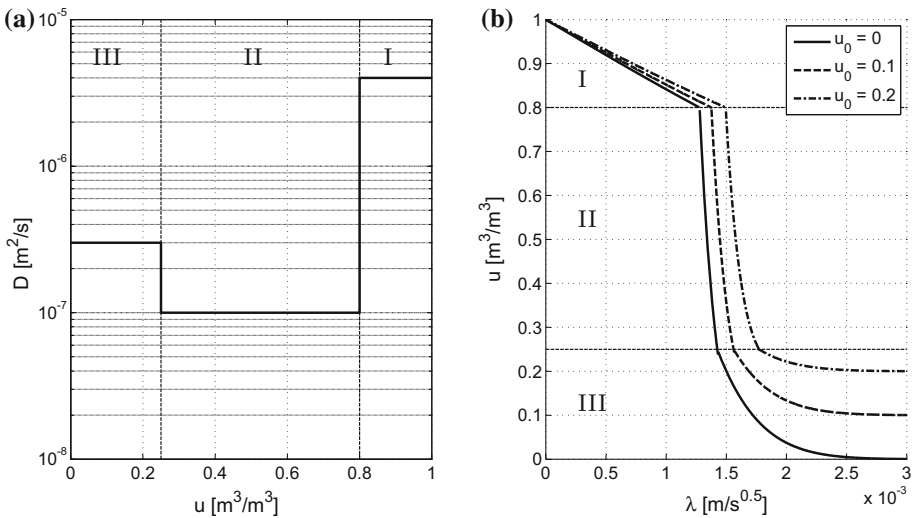

Fig. 5 a Diffusivity function $D(u)$ having a minimum in the middle region II; **b** resulting water content profiles for three different initial values of the volumetric moisture content u_0

In Fig. 6, the function $g(\lambda_1, \lambda_2)$ is shown for the three cases described above with $u_0 = 0$ (m^3/m^3). Since $\lambda_1 > \lambda_2$ holds, only the values under the main diagonal have been plotted.

The coefficients λ_1^* and λ_2^* have been calculated by the MATLAB function `fminsearch`, based on the Nelder–Mead algorithm (Lagarias et al. 1998). This simplex-based algorithm falls in the class of direct search methods, i.e., uses only function values, without any derivative information. It has the advantage to be less time-consuming comparing to other direct search

Fig. 6 Contour lines of the function $g(\lambda_1, \lambda_2)$ for the three exemplary cases described above with $u_0 = 0$ (m^3/m^3). The minimum value $g(\lambda_1^*, \lambda_2^*) = 0$ is identified by a cross-symbol
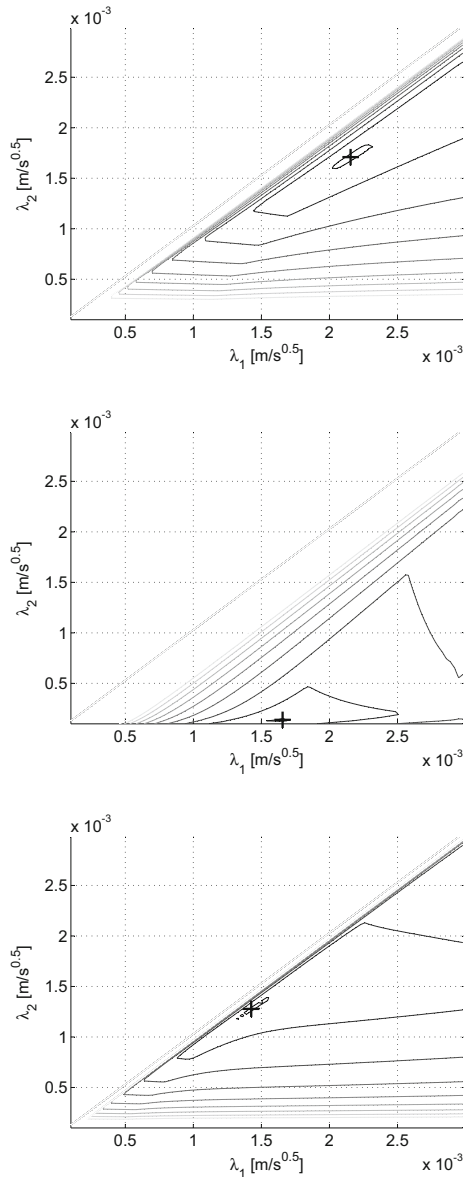
methods and produces significant improvement for the first few iterations. On the other hand, in some cases, it might fail to converge or converge to a non-minimizing point, as observed in Lagarias et al. (1998); McKinnon (1998).

In all examples considered in this study, the Nelder–Mead algorithm behaves indeed quite well. However, in case numerical issues should arise, the use of another algorithm for which convergence has been more generally proved [e.g., a pattern search algorithm (Torczon 1997)] is recommended.

5 Inverse Determination of the Diffusivity Function

In this section, a method is presented for inverse determination of the diffusivity function through a series of water uptake tests. Differently to other well-established techniques (Pel and Brocken 1996; Krus 1996; Carmeliet et al. 2004), the one proposed here does not require any knowledge of the water content distribution in the absorbing sample and can thus be advantageous in terms of costs and time.

Let us first observe that, according to the model introduced above, the following equation holds for an arbitrary initial water content u_0:

$$\frac{m(t) - m_0}{A\Psi\rho} \cong \int_0^\infty [u(t, x) - u_0]\, dx. \tag{24}$$

Here $m(t)$ denotes the total mass of moisture in the absorbing sample (kg) at the time t (s), m_0 the initial mass of moisture (kg), A the absorbing surface (m^2), Ψ the porosity ($-$) and ρ the density of water (kg/m^3). The function $u(t, x)$ is related to an arbitrary multiple step diffusivity described by Eq. (5). Note that the term $(m(t) - m_0)/(A\Psi\rho)$, on the left-hand side of Eq. (24), can be easily determined by weighting the moist sample during the absorption process (Plagge et al. 2005). Similarly, the initial water content u_0 can also be measured. Moreover, according to Fig. 1 and Eq. (10), we can write:

$$\int_0^\infty [u(t, x) - u_0]\, dx = \sum_{i=1}^n \int_{\lambda_i^* \sqrt{t}}^{\lambda_{i-1}^* \sqrt{t}} [u_i(t, x) - u_0]\, dx \tag{25}$$

with:

$$\int_{\lambda_i^* \sqrt{t}}^{\lambda_{i-1}^* \sqrt{t}} [u_i(t, x) - u_0]\, dx = \sqrt{\frac{4t D_i}{\pi}} \frac{\left(u_{i-1}^* - u_i^*\right)\left[e^{-\lambda_{i-1}^{*2}/(4D_i)} - e^{-\lambda_i^{*2}/(4D_i)}\right]}{\left[\operatorname{erf}\left(\frac{\lambda_{i-1}^*}{\sqrt{4D_i}}\right) - \operatorname{erf}\left(\frac{\lambda_i^*}{\sqrt{4D_i}}\right)\right]}$$
$$+ \sqrt{t}\left\{\left[\lambda_{i-1}^*\left(u_{i-1}^* - u_0\right) - \lambda_i^*\left(u_i^* - u_0\right)\right]\right\}. \tag{26}$$

In order to characterize the whole diffusivity function, a series of n water uptake tests is required. The parameters D_i are determined, starting from the highest water content level and decreasing step by step to the lowest one. The first test is hence performed with initial water content $u_0 = u_{n-1}^*$, to determine the diffusivity of the nearly saturated region D_n. Accordingly, Eq. (24) is written as follows:

$$\frac{m(t) - m_0}{A\Psi\rho} \cong \left(1 - u_{n-1}^*\right)\sqrt{\frac{4t D_n}{\pi}} \tag{27}$$

from which we immediately obtain:

$$D_n \cong \frac{\pi}{4t}\left[\frac{m(t) - m_0}{A\Psi\rho\left(1 - u_{n-1}^*\right)}\right]^2. \tag{28}$$

Each parameter $D_{k<n}$ can then be determined through a test performed with $u_0 = u_{k-1}^*$, by assuming that the diffusivity values at higher water content $D_{i>k}$ are already known. To this aim, it is worth to introduce the function f, defined as follows:

$$f(\lambda_k, \ldots, \lambda_i, \ldots, \lambda_{n-1}, D_k) = \left| \frac{m(t) - m_0}{A\Psi\rho} - \sum_{i=k}^{n} \int_{\lambda_i\sqrt{t}}^{\lambda_{i-1}\sqrt{t}} [u_i(t, x) - u_0] \, dx \right|$$
$$+ \sum_{i=k}^{n-1} |a_i - b_i|$$
(29)

where the coefficients a_i and b_i are given by Eq. (21) and $\lambda_{k-1} = \infty$. The unknown parameters λ_i^* and D_k can thus be determined by searching for the zero of the function f, i.e., by using one of the optimization techniques cited above (Lagarias et al. 1998; McKinnon 1998; Torczon 1997; Bonnans et al. 2006).

Note that the choice of the limit water contents u_i^* is arbitrary. If no information on the real diffusivity curve is available, a equally spaced distribution can be used. On the other hand, a finer partition at high water content might be advantageous, in case a nearly exponential behavior is expected. Obviously, the more tests are performed, the better the real diffusivity function can be approximated.

In order to test this inverse procedure, virtual experiments performed by means of numerical simulation are carried out. These simulated experiments shall substitute in this study real absorption tests. Hence, a diffusivity function with exponential behavior is assumed as input function of the simulation, while $n = 3$ is assigned in the multiple step model.

In the first instance, three equal water content regions, delimited by $u_1^* = 1/3$ and $u_2^* = 2/3$, are considered. The step function resulting from the inverse method and the exponential curve (i.e., input function) are shown in Fig. 7a, while in Fig. 7b the related water content profiles are plotted. It can be observed that, even if the fundamental absorption behavior is captured, the multiple step diffusivity underestimates the exponential curve in the middle water content range.

The accuracy can be significantly improved by adopting a finer partition at high water content, instead of equally spaced steps, as shown in Fig. 8 ($u_1^* = 0.6$; $u_2^* = 0.9$). In this plot, the multiple step diffusivity approximates quite well the exponential curve. Of course, further improvement could be obtained by increasing the number of steps.
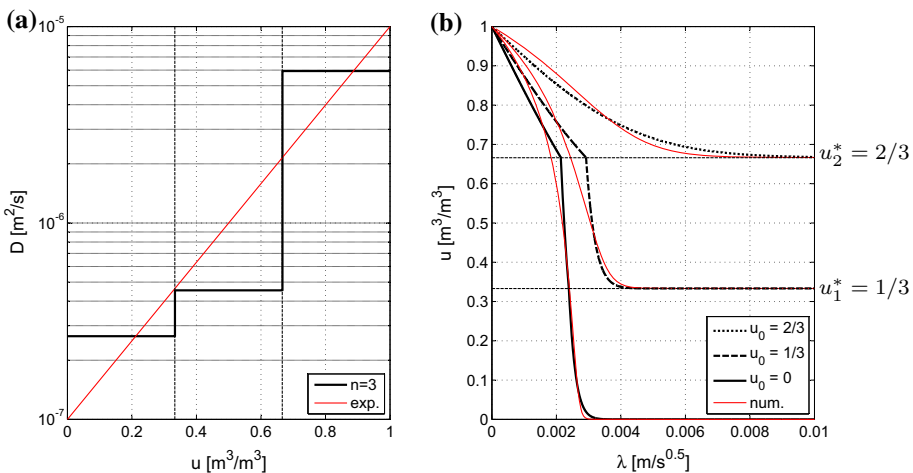

Fig. 7 Equally spaced partition: **a** diffusivity function $D(u)$; **b** water content profiles for three different initial values of the volumetric moisture content u_0
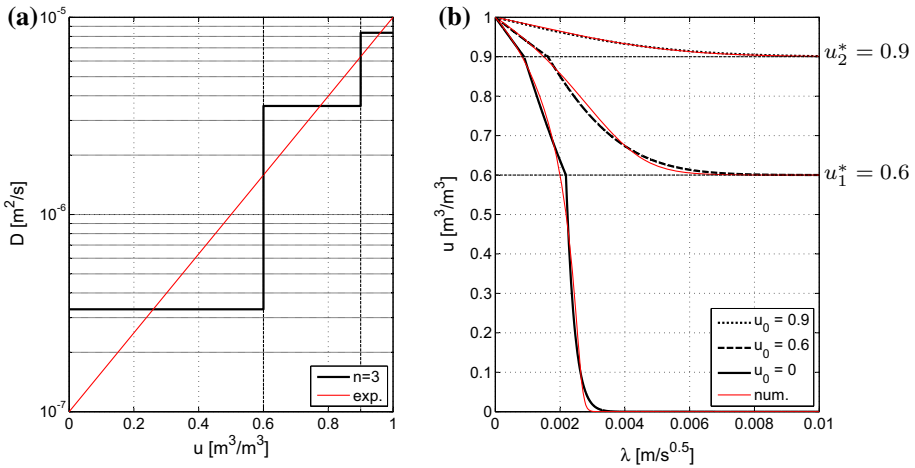
Fig. 8 Partition presenting finer steps at high water content: **a** diffusivity function $D(u)$; **b** water content profiles for three different initial values of the volumetric moisture content u_0

6 Conclusions

In this paper, an analytical solution for the problem of moisture absorption in homogeneous, capillary active materials is presented. The problem is solved by assuming the diffusivity as a multiple step function of the moisture content. While other analytical solutions available in the literature are accurate only for certain diffusivity functions, the one proposed here is applicable for an arbitrary diffusivity curve, and hence can be used to predict a large variety of absorption behaviors. The proposed solution can also be used for the inverse determination of the diffusivity function via water uptake tests, as explained in the last part of the paper. This inverse technique has been tested through simulated experiments with promising results and is now ready to be applied in the laboratory.

References

Barták, J., Herrmann, L., Lovicar, V., Vejvoda, O.: Partial Differential Equations of Evolution. Ellis Horwood Series in Mathematics and its Applications. Ellis Horwood, New York (1991)

Bianchi Janetti, M., Wagner, P.: Analytical model for the moisture absorption in capillary active building materials. Build. Environ. **126**, 98–106 (2017)

Bianchi Janetti, M., Carrubba, T.A., Ochs, F., Feist, W.: Heat flux measurements for determination of the liquid water diffusivity in capillary active materials. Int. J. Heat Mass Transf. **97**, 954–963 (2016)

Bonnans, J.-F., Gilbert, J., Lemarechal, C., Sagastizábal, C.: Numerical Optimization: Theoretical and Practical Aspects, 2nd edn. Springer, Berlin (2006)

Carmeliet, J., Hens, H., Roels, S., Adan, O., Brocken, H., Cerny, R., Pavlik, Z., Hall, C., Kumaran, K., Pel, L.: Determination of the liquid water diffusivity from transient moisture transfer experiments. J. Build. Phys. **27**(4), 277–305 (2004)

Carmeliet, J., Janssen, H., Derluyn, H.: An improved moisture diffusivity model for porous building materials. In: Meinhold, U., Petzold, H. (eds.) Proceedings of the 12th Symposium for Building Physics, pp. 228–235. Dresden, Germany, 29–31 March (2007)

Crank, J.: Diffusion in media with variable properties. Part III.—Diffusion coefficients which vary discontinuously with concentration. Trans. Faraday Soc. **47**, 450–461 (1951)

Crank, J.: The Mathematics of Diffusion. Clarendon Press, Oxford (1975)

Derluyn, H., Griffa, M., Mannes, D., Jerjen, I., Dewanckele, J., Vontobel, P., Sheppard, A., Derome, D., Cnudde, V., Lehmann, E., Carmeliet, J.: Characterizing saline uptake and salt distributions in porous limestone with neutron radiography and X-ray micro-tomography. J. Build. Phys. **36**(4), 353–374 (2013)

Gummerson, R.J., Hall, C., Hoff, W.D.: Water movement in porous building materials-II. Hydraulic suction and sorptivity of brick and other masonry materials. Build. Environ. **15**(2), 101–108 (1980)

Häupl, P., Grunewald, J., Fechner, H., Stopp, H.: Coupled heat air and moisture transfer in building structures. Int. J. Heat Mass Transf. **40**(7), 1633–1642 (1997)

Hristov, J.: Integral solutions to transient nonlinear heat (mass) diffusion with a power-law diffusivity: a semi-infinite medium with fixed boundary conditions. Heat Mass Transf. Waerme- und Stoffuebertragung **52**(3), 635–655 (2016)

Janssen, H.: Simulation efficiency and accuracy of different moisture transfer potentials. J. Build. Perform. Simul. **7**(5), 379–389 (2013)

Krus, M.: Moisture Transport and Storage Coefficients of Porous Mineral Building Materials–Theoretical Principles and New Test Methods. Fraunhofer IRB Verlag, Stuttgart (1996). ISBN 3-8167-4535-0

Künzel, H., Kiessl, K.: Calculation of heat and moisture transfer in exposed building components. Int. J. Heat Mass Transf. **40**, 159–167 (1996)

Lagarias, J., Reeds, J.A., Wright, M.H., Wright, P.E.: Convergence properties of the nelder–mead simplex method in low dimensions. SIAM J. Optim. **9**(1), 112–147 (1998)

Lockington, D.: Estimating the sorptivity for a wide range of diffusivity dependence on water content. Transp. Porous Media **10**(1), 95–101 (1993)

McKinnon, K.I.M.: Convergence of the Nelder–Mead simplex method to a nonstationary point. SIAM J. Optim. **9**(1), 148–158 (1998)

Parlange, J.-Y., Hogarth, W., Parlange, M., Haverkamp, R., Barry, D., Ross, P., Steenhuis, T.: Approximate analytical solution of the nonlinear diffusion equation for arbitrary boundary conditions. Transp. Porous Media **30**(1), 45–55 (1998)

Pel, L., Brocken, H.: Determination of moisture diffusivity in porous media using moisture concentration profiles. Int. J. Heat Mass Transf. **39**(6), 1273–1280 (1996)

Plagge, R., Scheffler, G., Grunewald, J.: Automatic measurement of water uptake coefficient of building materials. In: The 7th Symposium on Building Physics in the Nordic Countries, Reykjavík (2005)

Roels, S., Carmeliet, J.: Analysis of moisture flow in porous materials using microfocus X-ray radiography. Int. J. Heat Mass Transf. **49**(25–26), 4762–4772 (2006)

Roels, S., Carmeliet, J., Hens, H.: Modelling undersaturated moisture transport in heterogeneous limestone. Transp. Porous Media **52**(3), 333–350 (2000)

Torczon, V.: On the convergence of pattern search algorithms. SIAM J. Optim. **7**(1), 1–25 (1997)

Van Schijndel, A.W.M.: Integrated modeling of dynamic heat, air and moisture processes in buildings and systems using SimuLink and COMSOL. Build. Simul. **2**, 143–155 (2009)

Zhou, C.: General solution of hydraulic diffusivity from sorptivity test. Cem. Concr. Res. **58**, 152–160 (2014)

Zimmerman, R.W., Bodvarsson, G.S.: An approximate solution for one-dimensional absorption in unsaturated porous media. Water Resour. Res. **25**(6), 1422–1428 (1989)

Zimmerman, R.W., Bodvarsson, G.S.: A simple approximate solution for horizontal infiltration in a Brooks–Corey medium. Transp. Porous Media **6**(2), 195–205 (1991)